Many roads to success: alternative routes to building an economic shell in land snails

Barna Páll-Gergely, András Á. Sipos, Mathias Harzhauser, Aydın Örstan, ViolaWinkler, Thomas A. Neubauer

DOI
https://doi.org/10.1093/evolut/qpae018

Evolution, 2024, **XX(XX)**, 1–9
https://doi.org/10.1093/evolut/qpae018
Advance access publication 29 January 2024
Brief Communication

OXFORD

Many roads to success: alternative routes to building an economic shell in land snails

Barna Páll-Gergely[1], András Á. Sipos[2,3], Mathias Harzhauser[4,5], Aydın Örstan[6], Viola Winkler[4,7], Thomas A. Neubauer[8,9]

[1]Plant Protection Institute, HUN-REN Centre for Agricultural Research, Budapest, Hungary
[2]HUN-REN-BME Morphodynamics Research Group, Budapest University of Technology and Economics, Budapest, Hungary
[3]Department of Morphology and Geometric Modeling, Budapest University of Technology and Economics, Budapest, Hungary
[4]Geological-Paleontological Department, Natural History Museum, Vienna, Austria
[5]Institut für Erdwissenschaften, Bereich Geologie und Paläontologie, Universität Graz, Graz, Austria
[6]Section of Mollusks, Carnegie Museum of Natural History, Pittsburgh, PA, USA
[7]Central Research Laboratories, Natural History Museum Vienna, Vienna, Austria
[8]SNSB—Bavarian State Collection for Paleontology and Geology, Munich, Germany
[9]Naturalis Biodiversity Center, Leiden, The Netherlands

Corresponding authors: Plant Protection Institute, HUN-REN Centre for Agricultural Research, Herman Ottó út 15, Budapest, 1022, Hungary. Email: pallgergely2@gmail.com; HUN-REN-BME Morphodynamics Research Group, Budapest University of Technology and Economics, Műegyetem rkp. 1–3, Budapest, Hungary. Email: siposa@eik.bme.hu
B.P-G. and A.A.S. contributed equally.

Abstract

Land snails exhibit an extraordinary variety of shell shapes. The way shells are constructed underlies biological and mechanical constraints that vary across gastropod clades. Here, we quantify shell geometry of the two largest groups, Stylommatophora and Cyclophoroidea, to assess the potential causes for variation in shell shape and its relative frequency. Based on micro-computed tomography scans, we estimate material efficiency through 2D and 3D generalizations of the isoperimetric ratio, quantifying the ratios between area and perimeter of whorl cross-sections (2D) and shell volume and surface (3D), respectively. We find that stylommatophorans optimize material usage through whorl overlap, which may have promoted the diversification of flat-shelled species. Cyclophoroids are bound to a circular cross-section because of their operculum; flat shells are comparatively rare. Both groups show similar solutions for tall shells, where local geometry has a smaller effect because of the double overlap between previous and current whorls. Our results suggest that material efficiency is a driving factor in the selection of shell geometry. Essentially, the evolutionary success of Stylommatophora likely roots in their higher flexibility to produce an economic shell.

Keywords: shell geometry, shell shape, isoperimetric ratio, Cyclophoroidea, Stylommatophora

Introduction

How distantly related groups evolve in response to similar environmental factors is a fundamental topic of evolutionary biology (e.g., Hedenström et al., 2009; Zhou et al., 2015). A prime example is the conquest of land by originally marine animal groups that involves adaptation to an environment with different gravitational conditions and a higher risk of desiccation (Little, 1990). Among mollusks, Gastropoda (snails and slugs) represents the only class that could colonize terrestrial habitats. Of the approximately thirty land invasions documented in the history of Gastropoda (Vermeij & Watson-Zink, 2022), two clades comprise the vast majority of the nearly 30,000 known extant terrestrial species (MolluscaBase, 2023; Rosenberg et al., 2022)—Cyclophoroidea and Stylommatophora.

These two groups differ markedly in the number of known species, biology, habitat preference, and distribution. Stylommatophora comprise 22,356 extant species (Supplementary Table S1), are hermaphroditic, have a worldwide distribution, and occur in a great variety of habitats (Ponder et al., 2020; Schilthuizen et al., 2005). Cyclophoroidea, in turn, encompass 3,671 species today (Supplementary Table S1), have a gonochoric mode of reproduction, and are mostly restricted to the tropics and subtropics (Ponder et al., 2020; Schilthuizen et al., 2005). In Stylommatophora, the mantle collar is fused to the snail's neck, with only a small hole (pneumostome) serving as a passage during respiration, while in Cyclophoroidea the entire pallial surface is exposed to the air, which likely provides poorer water retention for the animal (Simone, 2022; Solem, 1974).

Besides differences of the soft body, cyclophoroideans and stylommatophorans differ fundamentally in the way their shells are constructed during ontogeny. Cyclophoroid shells have whorls with round cross-sections that touch the previous whorls only in a single point (or short curve segment; Figure 1A). This is associated with the presence of a usually circular operculum, a trapdoor-like structure that seals the aperture

Received September 13, 2023; revisions received January 15, 2024; accepted January 25, 2024
Associate Editor: Brian Sidlauskas; Handling Editor: Miriam Zelditch

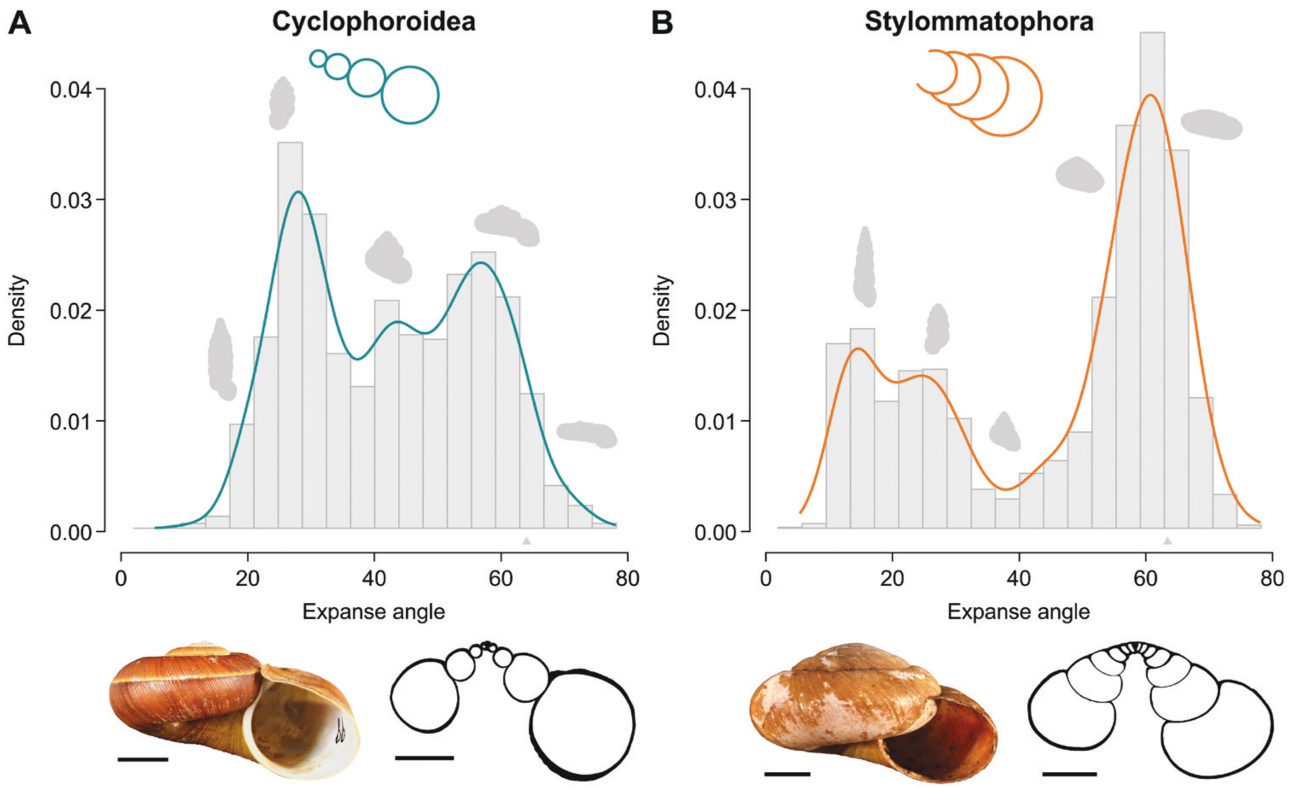

Figure 1. Shell shape distributions for Cyclophoroidea (A) and Stylommatophora (B). Histograms and Kernel density estimates are based on the expanse angle ε (see *Materials and methods* for details) calculated from measurements of 6,332 species and were scaled to have an equal area in both groups. Note particularly the different relative abundances of globular shells (expanse angle ~45°) in the two groups. The schematic sketches indicate the different growth types of Cyclophoroidea and Stylommatophora. Example shell shapes are indicated in gray and are derived from Stanisic et al. (2010) and Tongkerd et al. (2023). Illustrations in the bottom row show examples for each group, that is, the cyclophoroid *Incidostoma incomptum* (G. B. Sowerby I, 1850) and the stylommatophoran *Turcozonites megistus* (Rolle, 1894), including µCT scans. The two species have similar expanse angles (63.43° and 64.00°, respectively; marked by gray arrows below histograms), but differ markedly in their whorl architecture. Scale bars equal 5 mm. See also Supplementary Figure S3 for subsampling results and Supplementary Table S2 for the underlying data set.

when the snail withdraws its body into the shell (Páll-Gergely et al., 2016). Stylommatophorans, in contrast, have no opercula and their whorl cross-section consists of open curves, that is, the previously external surface becomes a part of the internal wall as the shell is produced (Figure 1B).

A further difference between the two groups is the relative abundance of shell shape types. The majority of stylommatophoran species have flat (low-spired) or tall (high-spired) shells, while globular shells with close-to-equal diameter and height are scarce (Cain, 1977; Cowie, 1995; Nekola, 2014; Páll-Gergely et al., 2023; Figure 1B). This bimodality has been attributed to mechanical reasons, namely, the difficulties in balancing a globular shell, making it more favorable to carry a flat shell or to drag a tall one (Cain, 1977; Okajima & Chiba, 2009, 2011, 2012). On the contrary, among cyclophoroidean snails, the globular shape is more common than among stylommatophorans, and flat shells are comparatively rarer than tall ones (Cain, 1978; Figure 1A).

Previous hypotheses aimed at explaining the differential evolutionary success of Cyclophoroidea and Stylommatophora in terms of species diversity and distribution range by differences in the anatomy of the breathing apparatus (Solem, 1974) or feeding behavior (Cain, 1978), yet without providing convincing support. Here, we take an alternative approach and hypothesize that different ways of constructing the shell and the related efficiency of material usage, which are mirrored in the observed differences in shell shape distribution patterns, may be a driving force behind the success of Stylommatophora. We use 3D data sets from computed tomography (CT) scans of 39 shells covering a large variety of growth forms across Cyclophoroidea and Stylommatophora to assess the relationship between growth type and material usage to evaluate differences in the efficiency of shell construction among the two groups. We compare both the local (2D) and global (3D) effectiveness in material usage of the shells to evaluate different growth strategies among the two groups.

Materials and methods

Taxon selection

We aimed to cover the morphological, systematic, and geographic variability of stylommatophoran and cyclophoroidean shells as broadly as possible. We selected 15 cyclophoroidean and 24 stylommatophoran shells from a wide range of families (6 in Cyclophoroidea and 16 in Stylommatophora) and geographical origins (Europe, Americas, Australia, and Asia). The data set includes shells of variable shapes (flat to high-spired), umbilical types (narrow to wide), and aperture shapes (rounded to crescent-shaped in stylommatophorans). We focused on species with no or only minimal apertural barriers to avoid any influence on the calculations. All material is stored in the collection of the Natural History Museum Vienna and the private collection of the first author (Supplementary Table S3).

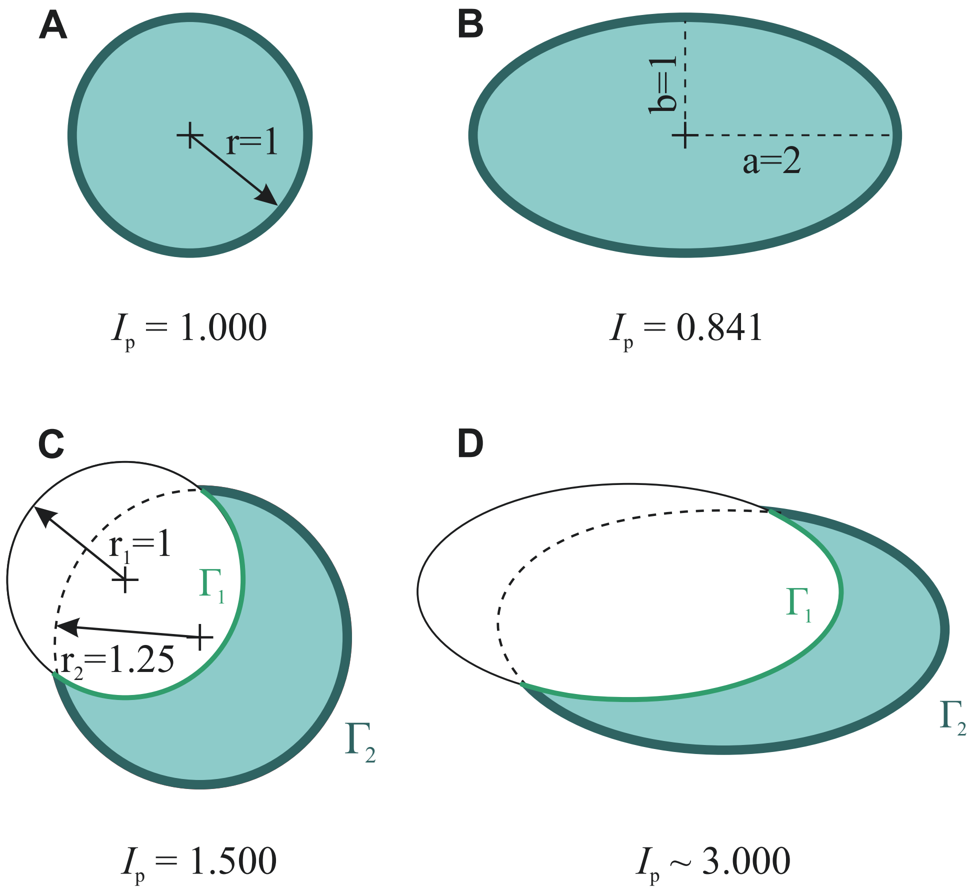

Figure 2. The isoperimetric ratio I_p^{2D} of different closed (A, B) and open curves (C, D). (C) I_p^{2D} for a circle with radius r_2 = 1.25 overlapped by a smaller circle with radius r_1 = 1.00. Note that while closed curves produce $I_p^{2D} \leq 1$ (A, B), the isoperimetric ratio of shapes created by overlap (C, D) can exceed 1.

The shells were imaged using X-ray microcomputed tomography (microCT; YXLON FF35 CT, FXE transmission beam, Y.Panel 4343 CT flat panel detector) at the Natural History Museum Vienna, Austria. See Supplementary Material for details.

Quantifying shell morphology

As we pointed out in the Introduction, creating the cyclophoroidean shell requires the production of a circular cross-section, which entails that subsequent whorls touch only in a single point or short curve segment at best (Figure 1). The cross-section of the stylommatophoran shell consists of open curves, that is, the previously external surface becomes internal as the shell is gradually produced. Assuming a constant thickness for the shell, we postulate that surrounding a unit volume with a smaller surface area is more optimal. This idea has a long track record in the geometric analysis of gastropod shells (Heath, 1985; Okabe & Yoshimura, 2017; Raup, 1966). However, the cited solutions either use dimensional parameters, such as the surface-to-volume (or perimeter-to-area) ratio (Heath, 1985), or uses the aspect ratio of the bounding box (Raup, 1967) to study the relation between the volume and the surface area of the shell. Note, that although the aspect ratio is a dimensionless parameter, it is a poor shape descriptor in cases, where the surface area and/or volume is tackled (Domokos et al., 2014). Another study traces aperture profiles through ontogeny to model gastropod shell form (Liew & Schilthuizen, 2016), but this approach does not allow assessing the global geometry and material usage, respectively. To characterize the volume that is enclosed by unit surface area, we propose to generalize the widely used isoperimetric ratio (Blåsjö, 2005) in such a way that new surface area needed to enclose the volume is distinguished from surfaces already existing at the time of construction. Using this nondimensional quantity eliminates the size effect inherent to any dimensional quantity. Moreover, many studies are based on the assumption of a circular cross-section and its affine transformations (Okabe & Yoshimura, 2017; Raup, 1966). Computed tomography scanning makes such a simplification obsolete; the cross-section can be directly extracted from the scan and quantified geometrically (Liew & Schilthuizen, 2016).

In the first step, we quantify the overlap of successive whorls. When the shell grows, new material is gradually added to the perimeter of the actual aperture (Okabe & Yoshimura, 2017); hence, vertical cross-sections of the whorls are simple but powerful descriptors of the spatial shape. The isoperimetric ratio associated with the cross-section of a whorl is defined as follows. Let Γ denote a closed, nonintersecting curve representing the cross-section. Let Γ_1 and Γ_2 be subsets of Γ such that $\Gamma = \Gamma_1 \cup \Gamma_2$ (Figure 2). Here, Γ_2 indicates the part of the curve needed to close Γ_1 (which already exists at the time of the production of the actual whorl). The generalized isoperimetric quotient is defined as

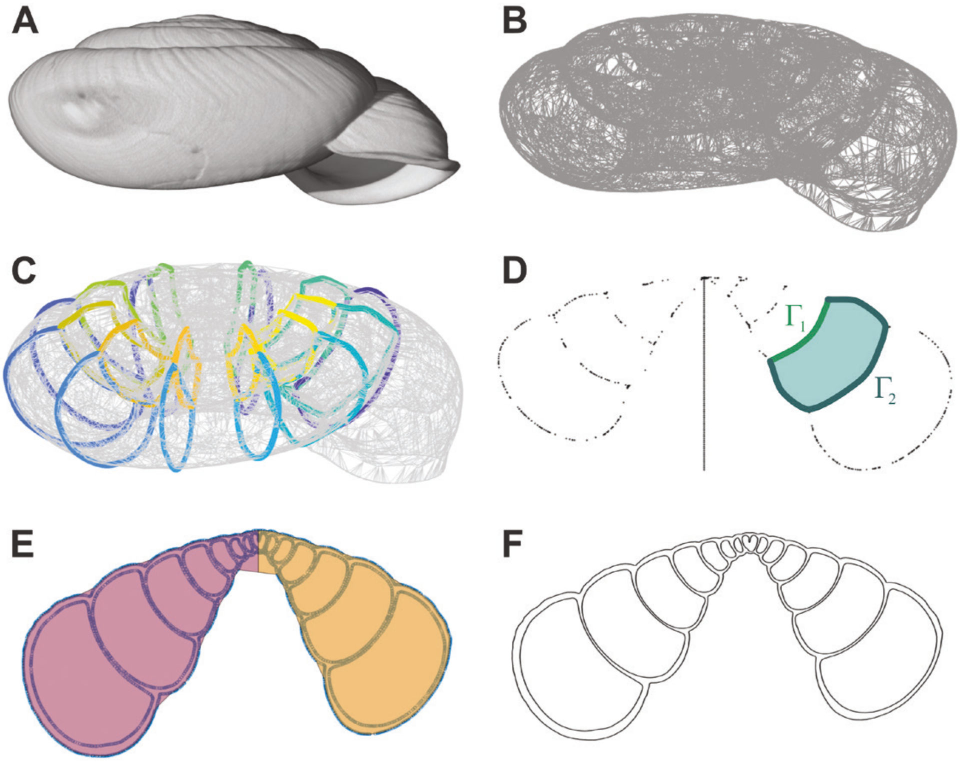

Figure 3. Steps of the computational data analysis demonstrated on the data set of *Aegista vermis* (Reeve, 1852). (A) Raw data of the CT scan. (B) Mid-surface obtained from the downsampled data. (C) Vertical cross-sections and identified closed curves (colored), starting a quarter whorl behind the aperture (see *Materials and methods* for details). (D) Curves Γ_1 and Γ_2 (dark curve) to calculate I_p^{2D} are identified in the vertical section. (E) The identified area used for the calculation of the volume element V_i. The colors are associated with the regions left and right of axis of rotation. In some cases, the boundary method in Matlab produces a slight offset at the deepest point of the umbilicus (as illustrated), but the resulting deviation of the total volume is negligible. (F) The same cross-section as in (E) was used to compute the surface area S. Note that the surface associated with the identified black curves is twice the mid-surface area S used in the computation of I_p^{3D}.

$$I_p := 4\pi \frac{A_\Gamma}{P_{\Gamma 2}^2}, \tag{1}$$

where A_Γ is the area enclosed by Γ and $P_{\Gamma 2}$ is the length of the curve segment Γ_2. Note that in case Γ_1 was empty, the formula recovers the isoperimetric quotient for closed curves. The prefactor 4π in *Equation 1* is applied to have $I_p = 1$ for a closed circle (Figure 2A). Note that, according to the isoperimetric inequality (Blåsjö, 2005), closed shapes other than a circle have $0 < I_p < 1$ (Figure 2B). However, if we take only a fragment of the perimeter into account in *Equation 1*, $I_p > 1$ becomes possible for any shape (Figure 2C and D). In the case of circular, overlapping cross-sections (as is approximated by Cyclophoroidea), I_p reaches a global optimum in dependence on the overlap (Supplementary Figure S1).

Similarly to the cross-section, the overall shell can be characterized by the spatial isoperimetric ratio I_p^{3D}. Assuming that the shell encloses a volume that extends until the plane of the aperture, the spatial isoperimetric ratio reads

$$I_p^{3D} := 6\sqrt{\pi} \frac{V}{\sqrt{S^3}}, \tag{2}$$

where V denotes the enclosed volume, and S is the surface area measured on the mid-surface of the shell. The prefactor $6\sqrt{\pi}$ in *Equation 2* is applied to have $I_p^{3D} = 1$ for a sphere. Here S contains all surfaces of the shell, regardless of whether it is considered external or internal. Assuming constant shell thickness, S reflects the material needed to establish the shell covering the internal volume V. Note that the I_p isoperimetric quotient in *Equation 1* (which will be henceforth denoted as I_p^{2D} to avoid confusion) characterizes the local geometry of a selected cross-section, while the spatial isoperimetric quotient I_p^{3D} is associated with the global shell shape. Regarding geometry, as we have demonstrated above, beneficial cross-sectional geometry and moderate overlap increase I_p^{2D} and, consequently, I_p^{3D}. On the other hand, the whorls' spatial arrangement also affects the value of I_p^{3D}. As demonstrated in the appendix (Supplementary Figure S2), whorls closer to the rotational axis of the shell (i.e., tall shells with narrow or no umbilicus) need less material because of the higher curvature of the whorl along its centerline.

Numerical analysis of the CT data

The point clouds of the CT scans (Figure 3A) with tens of thousand points were downsampled to 5,000–10,000 points with a uniform sampling of the data set. The global coordinate system was placed manually in such a way that the z-axis is aligned with the primary, rotational axis of the shell (i.e., the columella). (Due to the wide variety of shapes and the central axis's ambiguity, we decided on the manual placement instead of some algorithmic solution to have a meaningful result.) Next, a local averaging algorithm on point clouds was employed to determine the mid-surface of the shell, that is, the surface between the outer and inner shell layers (Figure 3B). A bias resulting from variability in shell thickness among species is thereby avoided. Altogether, 21 consecutive vertical cross-sections containing the global z-axis at an angular distance of 36° were generated from the 3D data set, covering a total of two entire whorls (720°) to account for variability through (late) ontogeny. The first vertical section is placed about a quarter whorl behind the aperture to avoid a bias from potential apertural inclination, expansion, or dentition. A path-following technique, implemented in Matlab v. 9.10.0.1649659 (MathWorks Inc., 2021), detects the closed curves associated with the whorl geometry inside the cross-sections (Figure 3C). For each cross-section, the outer part Γ_2 of the identified closed curve Γ is automatically predicted and manually corrected if needed to calculate I_p^{2D} (Figure 3D). The code is available at https://zenodo.org/records/10533717.

I_p^{3D} is computed for the entire shell. Altogether ten cross-sections with a vertical plane through the shell's axis of rotation are produced at an 18° angular distance. For each slice, the boundary of the shape is identified by the in-built boundary routine of Matlab (Figure 3E). The V_i volume associated with slice i is computed by considering the distance of the infinitesimal volume element from the axis of rotation. The overall volume V is obtained as the sum of V_i for each computed slice ($i = 1 \ldots 10$). Similarly, the length of the intersected shell material is summarized to estimate the surface S (*Equation 2*, Figure 3F).

Shell measurements for Stylommatophora and Cyclophoroidea

Data on shell height and diameter (Figure 1) were gathered from the literature. Focus was set on comprehensive catalogues (e.g., Nekola, 2014; Schileyko, 1998; Stanisic et al., 2010; Welter-Schultes, 2012) and generally a wide coverage of taxonomic groups and geographic regions, in order to capture overall shell shape distributions for the two groups reliably. Taxa were cross-checked with MolluscaBase for up-to-date systematic classification and status; subspecies and synonyms were not considered. In case of taxa with multiple subspecies, data were for the nominal subspecies. Species for which only measurements for shells with decollated apex were available were excluded, and so were species with uncoiled shells. Species with partly uncoiled last whorl (e.g., species of *Opisthostoma*) were only included if measurements for the regularly coiled part (without tube) were available. The final data set encompasses 6,332 species (2,460 Cyclophoroidea and 2,904 species Stylommatophora; Supplementary Table S2). Following Páll-Gergely et al. (2023), shell shape was quantified via the expanse angle ε, that is, the apex angle of a right triangle, of which the height and base correspond to shell height and diameter, respectively. Histograms with Gaussian Kernel density estimates were created in R v. 4.1.2 (R Core Team, 2021) with the package ggplot2 v. 3.3.5 (Wickham et al., 2021). To assess the robustness of the dataset, especially considering the undersampled stylommatophorans, we carried out a subsampling procedure. For both groups, random samples with various sampling fractions (0.25, 0.35, 0.45, 0.55, 0.65, and 0.75) were taken and Kernel density estimates were calculated. Each of these steps was repeated 999 times.

Results

We find that Cyclophoroidea and Stylommatophora show different solutions to build an economic shell. Species with flat shells (expanse angle $\varepsilon > 45°$) have on average higher I_p^{2D} values for stylommatophorans (1.511 ± 0.374) than for cyclophoroideans (1.278 ± 0.128), indicating a more efficient and close-to-optimal local shell geometry for the former group (Figure 4A, Supplementary Figure S1, Supplementary Table S3). Two flat-shelled stylommatophoran taxa constitute

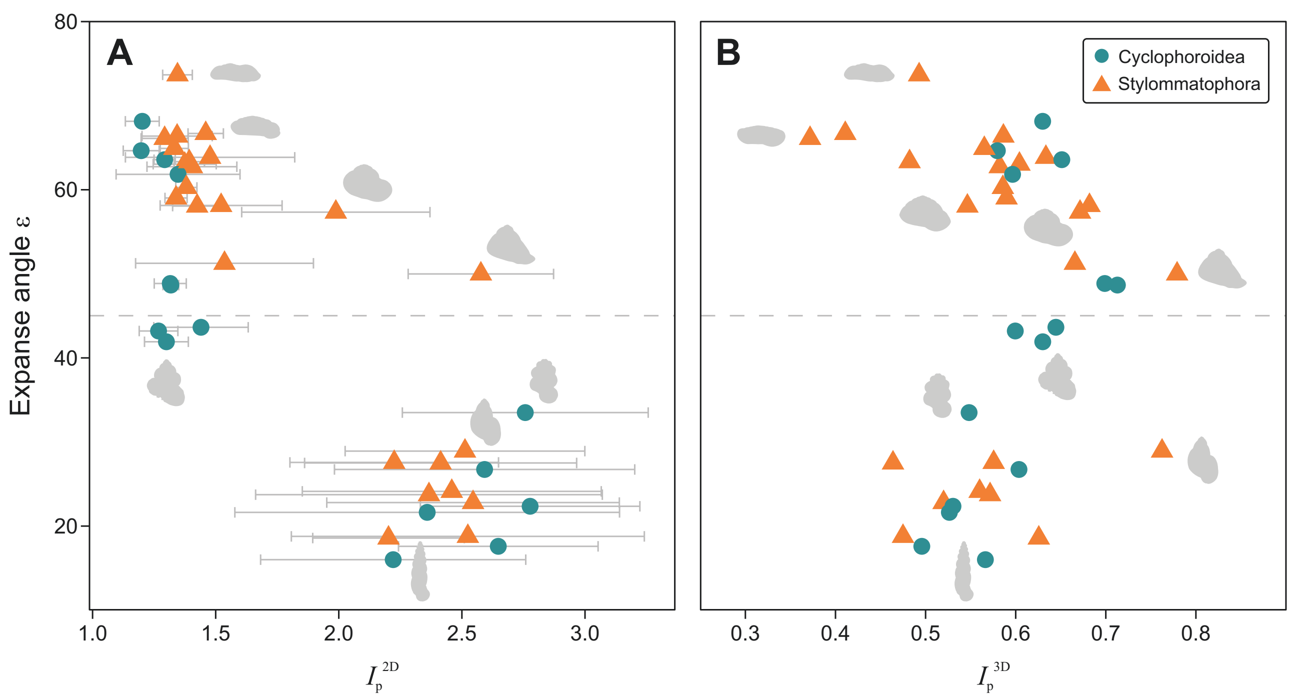

Figure 4. (A) Expanse angle ε versus isoperimetric ratio (I_p^{2D}), showing the variation of local geometry across different shell shapes. Error bars indicate standard deviations based on 21 cross-sections across two whorls. Note the differences between tall (ε < 45°) and flat (ε > 45°) shells in terms of average I_p^{2D} and its variability through ontogeny. (B) Expanse angle versus spatial isoperimetric ratio (I_p^{3D}), illustrating global material efficiency across shell shapes. Unlike in (A) I_p^{3D} varies distinctly less between tall and flat shells, for both Cyclophoroidea and Stylommatophora.

outliers with exceptionally high I_p^{2D} values, that is, *Calocochlea coccomelos princeps* (Reeve, 1854) (mean $I_p^{2D} = 1.987$) and *Acavus haemastoma* (Linnaeus, 1758) (mean $I_p^{2D} = 2.5768$). In terms of material efficiency, these taxa "overshoot" by producing shells with too much whorl overlap. For tall shells, in contrast, average I_p^{2D} hardly differs among the two groups (Figure 4A). Cyclophoroids reach a slightly higher average I_p^{2D} (2.559 ± 0.586) than Stylommatophora (2.406 ± 0.567), but the total ranges of values widely overlap (note that the three taxa with ε slightly below 45° are not considered tall but globular here). Moreover, I_p^{2D} varies considerably more throughout ontogeny than for flat shells (Figure 4A). This may at least partly be the result of the different ontogenetic developments of tall and flat shells. For example, juveniles of flat-shelled snails are always flat, while juveniles of tall forms can be both tall and flat (e.g., some species of Streptaxidae; Páll-Gergely et al., 2023; Rowson et al., 2010).

A very different picture is drawn by I_p^{3D} (Figure 4B). While there is slightly more variation among flat shells and Stylommatophora, group means are very similar across different shell shapes (Cyclophoroidea: 0.595 ± 0.068; Stylommatophora: 0.575 ± 0.099, Supplementary Table S3). This outcome suggests that while local geometry may be more or less beneficial depending on the type of whorl overlap, global geometry can be optimized independently through shell shape. In geometric terms, flat shells attain an ideal architecture by adjusting local geometry, while tall shells are already more optimally constructed since they have a reduced (narrower) umbilicus (or none at all) and thus utilize parts of the penultimate whorl when building the new whorl.

Discussion

Our results suggest that material efficiency is a driving factor in the selection of land snail shell geometry. Through an adaptation of the isoperimetric ratio, a commonly used parameter in analytic geometry, we show that different paths to success exist for the two largest clades of land snails, that is, Cyclophoroidea and Stylommatophora. The spatial isoperimetric ratio (I_p^{3D}) depends on two factors: the overlap between subsequent whorls and the distance of the cross-section from the axis of rotation. An economic shell geometry can therefore be approached by either having a tall shell with whorls touching as close as possible (i.e., closed or narrow umbilicus) or an optimal whorl overlap (i.e., an optimized I_p^{2D}).

In land snails, optimizing material usage (by maximizing the value of I_p^{3D}) underlies both geometric and biological constraints, which reflect the fundamental differences between Cyclophoroidea and Stylommatophora. Cyclophoroidean snails possess a usually circular operculum, a trapdoor-like structure that seals the aperture when the snail withdraws its body into the shell (thus the name, meaning "round-bearing") (Egorov, 2009, 2013). This tight sealing mechanism provides protection against predators and desiccation (Páll-Gergely et al., 2016; Rees, 1964). Stylommatophoran snails have no opercula and, thus, have to find alternative ways to avoid predation and desiccation, such as by minimizing the size of the aperture or building calcareous apertural barriers, permanent or temporary (Barnhard, 1983; Gittenberger, 1996; Solem, 1972), or pseudoopercula formed by the animal's foot (Solem et al., 1984). A potential link between shell geometry and these, partly very common, strategies is yet to be examined.

Because of the different geometric constraints, Cyclophoroidea and Stylommatophora find different solutions to approach an economic shell. Flat stylommatophorans improve the local geometry and whorl overlap, respectively, while cyclophoroideans seem more or less bound to a circular cross-section to fit the operculum (Figure 4A); accordingly, flat shells are considerably rarer (Cain, 1977, this study; Figure 1). In contrast, both groups show similarly beneficial solutions for tall shells, where the whorls are as close as possible to the axis of rotation (i.e., the columella) and the local geometry has a smaller effect because of the double overlap between former and actual whorls.

An intermediate, near-globular shell shape is rarely found in land snails because it is unfavorable for mechanical reasons. Studies have shown that a globular shell is difficult to balance on the soft body (Cain, 1977; Goodfriend, 1986; Okajima & Chiba, 2012). Despite that restriction, a near-globular shell is considerably more frequent in Cyclophoroidea than in Stylommatophora (Cain, 1977; Figure 1). One potential reason involves an increased mechanical stability of a globular shell, making it more resistant to crushing by predators (Okajima & Chiba, 2012; Verhaegen et al., 2019). On the other hand, a near-globular shell coincides with a narrower umbilicus and thus a more efficient shell geometry, since less new material has to be used to build the current whorl (Supplementary Figure S2). For a cyclophoroid, being a coiled tube with a circular cross-section, this is virtually the only way of saving material. Considering the relative abundance of that shell form in cyclophoroids, it seems likely that building an economic shell overrules difficulties of balancing a globular shell in terms of selection pressure. Perhaps also the columellar muscle system of operculate snails, which extends until the operculum, allows a wider range of mechanical possibilities compared to stylommatophorans, where the muscle is mostly restricted to the anterior and middle part of the body (Ponder et al., 2020: figs 3.51–3.52).

Nonetheless, said mechanical constraint could explain the general conservatism of shell shapes in systematic groups. Despite the advantage of having a tall shell, species with high-spired shells are exceptionally rare in groups typically characterized by flat shells. The gradual evolution from flat to tall shells and vice versa is probably selected against due to the unfavorable balance of globular shells. Cases of "crossing the adaptive valley" (Gittenberger, 2010), that is, abrupt (non-gradual) shifts from flat to high-spired shells, are known but too rare to be adaptive (Asami et al., 1998). Examples include the helicid genus *Cylindrus* (Cadahía et al., 2013; Zopp et al., 2017) and the genera *Pseudobuliminus*, *Sinorachis*, and *Stenogyropsis* in Camaenidae (Chen et al., 2022; Hirano et al., 2014; Wu et al., 2019).

The trade-off between material efficiency and geometric and biological constraints is probably the reason for the observed variability in I_p^{2D} and I_p^{3D} across species as well as for the presence of outliers. Stylommatophora show cases where the optimal whorl overlap is sacrificed for a narrower aperture, probably as a function of predation pressure. One such example is the hygromiid *Perforatella bidentata* (Gmelin, 1791), which is regularly preyed upon by the gastrodontid *Aegopinella nitidula* (Draparnaud, 1805). In addition to apertural barriers, the species exhibits a narrow whorl cross-section (Myzyk, 2014).

In case of flat shells, the alternative ways of constructing a shell of the two groups comes with implications for material usage. Assuming constant shell thickness, cyclophoroids require on average more calcium carbonate than do stylommatophorans to build a shell of a given size and shape (compare Figure 4A). Carbonate availability may be a limiting factor in some places, which may exert an evolutionary disadvantage for cyclophoroids. However, little is known about the relative abundance of cyclophoroids versus stylommatophorans with respect to habitat conditions. At least for certain regions cyclophoroids are known to be more associated with limestone habitats than Stylommatophora (Schilthuizen et al., 2005).

Overall, the flexibility of the stylommatophoran architecture and their potential to navigate between an optimal relationship of shell shape and whorl overlap, always in dependence of biological and mechanical constraints (e.g., shell balance, predation, and desiccation avoidance), have made them the more successful group. Stylommatophora include today more than six times as many species as Cyclophoroidea (Supplementary Table S1), have a wider geographic distribution, and occupy a greater variety of habitats (MolluscaBase, 2023; Solem, 1974). Their flexibility has opened adaptive pathways that result in various lifestyles, such as carnivorous behavior, shell reduction, and complex apertural structure, none of which occurs in cyclophoroids (Barker, 2004; Cameron, 2016; Solem, 1974). Our interpretation of their evolutionary success is supported by a more or less continuous increase of the relative diversity of stylommatophorans through Earth history (Supplementary Figure S4). While cyclophoroids were relatively diverse in the Mesozoic (e.g., Balashov, 2021), they were soon outcompeted by stylommatophorans (Harzhauser & Neubauer, 2021; MolluscaBase, 2023). In addition, Stylommatophora are the much older group, dating back to the Late Carboniferous, while the oldest Cyclophoroidea are of Jurassic age (Neubauer, 2023).

In conclusion, our approach to evaluate and compare shell geometries from an economic point of view using the isoperimetric ratio provides new insights on the evolution of shell types in land snails. We show that Cyclophoroidea and Stylommatophora have come up with alternative solutions to construct a shell efficiently, while mechanical and biological factors constrain the available possibilities for both groups in different ways. For cyclophoroids, the operculum limits the whorl cross-section to a circle—economic solutions involve reducing the umbilicus and/or producing tall shells. The non-operculate stylommatophorans, in turn, are not bound to a particular whorl cross-section and can optimize shell material usage by finding the ideal whorl overlap. In particular, this allowed them to evolve a higher relative diversity of flat-shelled species. While previously mentioned differences in breathing apparatus and feeding (Cain, 1978; Solem, 1974) certainly play a role, we propose that these fundamental differences in the ways to construct an efficient shell—and particularly the higher flexibility of the stylommatophoran shell—explain the greater evolutionary success of the Stylommatophora.

As representatives of operculate terrestrial snails, we here only analyzed shells of Cyclophoroidea, which is the largest monophyletic group of terrestrial Caenogastropoda. Since the shell shape types and mechanical constraints due to a circular operculum are similar in the second largest group, the Littorinoidea (Supplementary Table S1; Cain, 1978), we expect that our explanation model also applies to that group. The application of our approach is not limited to terrestrial taxa but may be expanded towards freshwater and marine groups, which underlie different geometric and biological constraints. Future studies may include such constraints in their mathematical models and moreover consider shell thickness variation across species, the effect of apertural barriers, as well as habitat conditions such as local availability of calcium carbonate.

Supplementary material

Supplementary material is available online at *Evolution*.

Data availability

Matlab code used for the computations are available here: https://zenodo.org/records/10533717. CT files are available here: https://doi.org/10.57756/g7jjq4

Author contributions

B.P.G., A.A.S, M.H., and T.A.N. designed the study; B.P.G., T.A.N., and A.Ö. collected data; V.W. performed the CT scans; A.A.S., T.A.N., and A.Ö analyzed the data; B.P.G., A.A.S, and T.A.N. led the writing of the manuscript, with contributions from all authors; B.P.G., A.A.S, and T.A.N. designed the artwork. All authors contributed to the interpretation and approved the final version of the manuscript.

Funding

This study was supported by the Hungarian Research Fund grants OTKA FK 135262 (B.P.G.) and OTKA K134199 (A.A.S.), the Bolyai Research Scholarship of the Hungarian Academy of Sciences for B.P.G., and the National Research, Development, and Innovation Fund of Hungary under grant TKP2021-NVA-02 (A.A.S.).

Conflict of interest: All authors declare that they have no conflicts of interest.

Acknowledgments

We are grateful to Anita Eschner for her help in selecting shells for CT scanning, to Ivo Gallmetzer in his help in photographing, to Jeff Nekola for sharing the size data set for North American land snails, and to Peter Wagner and an anonymous reviewer for their comments on the manuscript.

References

Asami, T., Cowie, R. H., & Ohbayashi, K. (1998). Evolution of mirror images by sexual asymmetric mating behavior in hermaphroditic snails. *American Naturalist*, *152*(2), 225–236. https://doi.org/10.1086/286163

Balashov, I. (2021). An inventory of molluscs recorded from mid-Cretaceous Burmese amber, with the description of a land snail, *Euthema annae* sp. nov. (Caenogastropoda, Cyclophoroidea, Diplommatinidae). *Cretaceous Research*, *118*, 104676. https://doi.org/10.1016/j.cretres.2020.104676

Barker G. M. (2004). *Natural enemies of terrestrial molluscs*. CABI Publishing.

Barnhard, M. C. (1983). Gas permeability of the epiphragm of a terrestrial snail, *Otala lactea*. *Physiological Zoology*, *56*, 436–444. https://doi.org/10.1086/physzool.56.3.30152609

Blåsjö, V. (2005). The isoperimetric problem. *The American Mathematical Monthly*, *112*(6), 526–566. https://doi.org/10.1080/00029890.2005.11920227

Cadahía, L., Harl, J., Duda, M., Sattmann, H., Kruckenhauser, L., Fehér, Z., Zopp, L., & Haring, E. (2013). New data on the phylogeny of Ariantinae (Pulmonata, Helicidae) and the systematic position of *Cylindrus obtusus* based on nuclear and mitochondrial DNA marker sequences. *Journal of Zoological Systematics and Evolutionary Research*, *52*(2), 163–169. https://doi.org/10.1111/jzs.12044

Cain, A. J. (1977). Variation in the spire index of some coiled gastropod shells, and its evolutionary significance. *Philosophical Transactions of the Royal Society of London, Series B: Biological Sciences*, *277*(956), 377–428. https://doi.org/10.1098/rstb.1977.0026

Cain, A. J. (1978). The deployment of operculate land snails in relation to shape and size of shell. *Malacologia*, *17*(2), 207–221.

Cameron, R. (2016). *Slugs and snails*. Harper Collins Publishers.

Chen, Z.-Y., Huang, B., & Páll-Gergely, B. (2022). Exceptional among the exceptional: A new species of *Stenogyropsis* Möllendorff, 1899 (Eupulmonata: Camaenidae), with a review of the free last whorl in terrestrial gastropods. *Journal of Molluscan Studies*, *88*(3), eyac015. https://doi.org/10.1093/mollus/eyac022

Cowie, R. H. (1995). Variation in species diversity and shell shape in Hawaiian land snails: In situ speciation and ecological relationships. *Evolution*, *49*(6), 1191–1202. https://doi.org/10.1111/j.1558-5646.1995.tb04446.x

Domokos, G., Jerolmack, D. J., Sipos, A. A., & Török, A. (2014). How river rocks round: Resolving the shape-size paradox. *PLoS One*, *9*(2), e88657. https://doi.org/10.1371/journal.pone.0088657

Egorov, R. V. (2009). *Treasure of Russian Shells; Supplement 3, A review of the genera of the recent terrestrial pectinibranch molluscs (synopsis mainly based on published data); Part II, Littoriniformes: Hainesiidae, Aciculidae, Cyclophoridae, Craspedopomatidae*. Colus-Doverie, Roman Egorov.

Egorov, R. V. (2013). *Treasure of Russian Shells. Supplement 3. A review of the genera of the terrestrial pectinibranch molluscs (synopsis mainly based on published data). Part III. Littoriniformes: Liareidae, Pupinidae, Diplommatinidae, Alycaeidae, Cochlostomidae*. Roman Egorov.

Gittenberger, E. (1996). Adaptations of the aperture in terrestrial gastropod-pulmonate snails. *Netherlands Journal of Zoology*, *46*, 191–205.

Gittenberger, E. (2010). Changes in shell shape. In C. Bakels, K. Fennema, W. A. Out, & C. Vermeeren (Eds.), *Of plants and snails: A collection of papers presented to Wim Kuijper in gratitude for forty years of teaching and identifying* (pp. 63–69). Sidestone Press.

Goodfriend, G. A. (1986). Variation in land-snail shell form and size and its causes: A review get access arrow. *Systematic Biology*, *35*(2), 204–223. https://doi.org/10.1093/sysbio/35.2.204

Heath, D. J. (1985). Whorl overlap and economical construction of the gastropod shell. *Biological Journal of the Linnean Society*, *24*(2), 165–174. https://doi.org/10.1111/j.1095-8312.1985.tb00167.x

Harzhauser, M., & Neubauer, T. A. (2021). A review of the land snail faunas of the European Cenozoic – composition, diversity and turnovers. *Earth-Science Reviews*, *217*, 103610. https://doi.org/10.1016/j.earscirev.2021.103610

Hedenström, A., Johansson, C., & Spedding, G. R. (2009). Bird or bat: Comparing airframe design and flight performance. *Bioinspiration & Biomimetics*, *4*(1), 015001. https://doi.org/10.1088/1748-3182/4/1/015001

Hirano, T., Kameda, Y., Kimura, K., & Chiba, S. (2014). Substantial incongruence among the morphology, taxonomy, and molecular phylogeny of the land snails *Aegista*, *Landouria*, *Trishoplita*, and *Pseudobuliminus* (Pulmonata: Bradybaenidae) occurring in East Asia. *Molecular Phylogenetics and Evolution*, *70*, 171–181. https://doi.org/10.1016/j.ympev.2013.09.020

Liew, T.-S., & Schilthuizen, M. (2016). A method for quantifying, visualising, and analysing gastropod shell form. *Plos One*, *11*(6), e0157069. https://doi.org/10.1371/journal.pone.0157069

Little, C. (1990). *The terrestrial invasion: An ecophysiological approach to the origins of land animals*. Cambridge University Press.

MathWorks, Inc. (2021). *MATLAB version: 9.10.0.1649659 (R2021a)*. The MathWorks, Inc.

MolluscaBase (2023). *MolluscaBase*. https://www.molluscabase.org. https://doi.org/10.14284/448

Myzyk, S. (2014). The predator *Aegopinella nitidula* (Draparnaud, 1805) and its prey *Perforatella bidentata* (Gmelin, 1791) (Gastropoda: Pulmonata). *Folia Malacologica*, *22*(3), 225–227. https://doi.org/10.12657/folmal.022.011

Nekola, J. C. (2014). Overview of the North American terrestrial gastropod fauna. *American Malacological Bulletin*, *32*(2), 225–235. https://doi.org/10.4003/006.032.0203

Neubauer, T. A. (2023). The fossil record of freshwater Gastropoda—A global review. *Biological Reviews*, *99*(1), 177–199. https://doi.org/10.1111/brv.13016

Okabe, T., & Yoshimura, J. (2017). Optimal designs of mollusk shells from bivalves to snails. *Scientific Reports*, *7*, 42445. https://doi.org/10.1038/srep42445

Okajima, R., & Chiba, S. (2009). Cause of bimodal distribution in the shape of a terrestrial gastropod. *Evolution*, *63*(11), 2877–2887. https://doi.org/10.1111/j.1558-5646.2009.00780.x

Okajima, R., & Chiba, S. (2011). How does life adapt to a gravitational environment? The outline of the terrestrial gastropod shell. *The American Naturalist*, *178*(6), 801–809. https://doi.org/10.1086/662674

Okajima, R., & Chiba, S. (2012). Adaptation from restricted geometries: The shell inclination of terrestrial gastropods. *Evolution*, *67*(2), 429–437. https://doi.org/10.1111/j.1558-5646.2012.01772.x

Páll-Gergely, B., Auffenberg, K., & Gojšina, V. (2023). A review of the Diapheridae of the Philippines (Gastropoda, Stylommatophora: Streptaxoidea). *Basteria*, *87*(2), 225–299.

Páll-Gergely, B., Naggs, F., & Asami, T. (2016). Novel shell device for gas exchange in an operculated land snail. *Biology Letters*, *12*(7), 20160151. https://doi.org/10.1098/rsbl.2016.0151

Páll-Gergely, B., Hunyadi, A., Vermeulen, J. J., Grego, J., Sutcharit, C., Reischuetz, A., Dumrongrojwattana, P., Botta-Dukat, Z., Örstan, A., Fekete, J., & Jochum, A. (2023). Five times over: 42 new *Angustopila* species highlight Southeast Asia's rich biodiversity (Gastropoda, Stylommatophora, Hypselostomatidae). *ZooKeys*, *1147*, 1–177. https://doi.org/10.3897/zookeys.1147.93824

Ponder, W. F., Lindberg, D. R., & Ponder, J. M. (2020). *Biology and evolution of the mollusca*. (Vol. *1*). CRC Press.

R Core Team. (2021). *R: A language and environment for statistical computing. Version 4.1.2*. R Foundation for Statistical Computing. https://www.r-project.org/

Raup, D. M. (1966). Geometric analysis of shell coiling: General problems. *Journal of Paleontology*, *40*(5), 1178–1190.

Raup, D. M. (1967). Geometric analysis of shell coiling: Coiling in ammonoids. *Journal of Paleontology*, *41*(1), 43–65.

Rees, W. J. (1964). A review of breathing devices in land operculate snails. *Proceedings of the Malacological Society of London*, *36*, 55–67.

Rosenberg, G., Auffenberg, K., Bank, R., Bieler, R., Bouchet, P., Herbert, D., Köhler, F., Neubauer, T. A., Neubert, E., Páll-Gergely, B., Richling, I., & Schneider, S. (2022). Adapting mark-recapture methods to estimating accepted species-level diversity: A case study with terrestrial Gastropoda. *PeerJ*, *10*, e13139. https://doi.org/10.7717/peerj.13139

Rowson, B., Warren, B. H., & Ngereza, C. F. (2010). Terrestrial molluscs of Pemba Island, Zanzibar, Tanzania, and its status as an 'oceanic' island. *ZooKeys*, *70*, 1–39. https://doi.org/10.3897/zookeys.70.762

Schileyko, A. A. (1998). Treatise on recent terrestrial pulmonate molluscs. Part 1. Achatinellidae, Amastridae, Orculidae, Strobilopsidae, Spelaeodiscidae, Valloniidae, Cochlicopidae, Pupillidae, Chondrinidae, Pyramidellidae. *Ruthenica*, *Supplement 2*, 1–2210.

Schilthuizen, M., Liew, T. -S., bin Elahan, B., & Lackmann-Ancrenaz, I. (2005). Effects of karst forest degradation on Pulmonate and Prosobranch land snail communities in Sabah, Malaysian Borneo. *Conservation Biology*, *19*(3), 949–954.

Simone, L. R. L. (2022). Why are pulmonates the most successful land snails? *Malacopedia*, *5*(3), 17–22.

Solem, A. (1972). Microarmature and barriers in the aperture of land snails. *The Veliger*, *15*, 81–87.

Solem, A. (1974). *The shell makers: Introducing mollusks*. John Wiley & Sons.

Solem, A., Tillier, S., & Mordan, P. (1984). Pseudooperculate pulmonate land snails from New Caledonia. *Veliger*, *27*, 193–199.

Stanisic, J., Shea, M., Potter, D., & Griffiths, O. (2010). *Australian land snails. Volume 1. A field guide to eastern Australian species*. Queensland Museum.

Tongkerd, P., Tumpeesuwan, S., Inkhavilay, K., Prasankok, P., Jeratthitikul, E., Panha, S., & Sutcharit, C. (2023). Systematic revision of the snorkel snail genus *Rhiostoma* Benson, 1860 (Gastropoda, Caenogastropoda, Cyclophoridae) with descriptions of new species. *ZooKeys*, *1142*, 1–144. https://doi.org/10.3897/zookeys.1142.90097

Verhaegen, G., Herzog, H., Korsch, K., Kerth, G., Brede, M., & Haase, M. (2019). Testing the adaptive value of gastropod shell morphology to flow: A multidisciplinary approach based on morphometrics, computational fluid dynamics and a flow tank experiment. *Zoological Letters*, *5*, 5. https://doi.org/10.1186/s40851-018-0119-6

Vermeij, G. J., & Watson-Zink, V. M. (2022). Terrestrialization in gastropods: Lineages, ecological constraints and comparisons with other animals. *Biological Journal of the Linnean Society*, *136*(3), 393–404. https://doi.org/10.1093/biolinnean/blac053

Welter-Schultes, F. W. (2012). *European non-marine molluscs, a guide for species identification*. Planet Poster Editions.

Wickham, H., Chang, W., Henry, L., Pedersen, T. L., Takahashi, K., Wilke, C., Woo, K., Yutani, H., & Dunnington, D. (2021). *ggplot2: Create Elegant Data Visualisations Using the Grammar of Graphics. R package version 3.3.5*. https://cran.r-project.org/web/packages/ggplot2/index.html

Wu, M., Chen, Z., & Zhang, L. (2019). Jawless land snail *Sinorachis*, a new bradybaenine genus from China (Eupulmonata, Camaenidae). *ZooKeys*, *893*, 51–67. https://doi.org/10.3897/zookeys.893.38445

Zhou, X., Seim, I., & Gladyshev, V. N. (2015). Convergent evolution of marine mammals is associated with distinct substitutions in common genes. *Scientific Reports*, *5*, 16550. https://doi.org/10.1038/srep16550

Zopp, L., Haring, E., Kruckenhauser, L., Schileyko, A., & Sattmann, H. (2017). Anatomical and morphological variation in the eastern Alpine endemic *Cylindrus obtusus* (Draparnaud, 1805) (Gastropoda: Helicidae). *Journal of Molluscan Studies*, *83*(3), 316–324. https://doi.org/10.1093/mollus/eyx022